J. Pharm. Pharmac., 1968, **20**, 255–268 Received November 13, 1967

Concentric cylinder creep investigation of pharmaceutical semi-solids

B. WARBURTON AND B. W. BARRY*

The rheological examination of pharmaceutical preparations has not often taken into account the contributions of viscoelasticity. Many semi-solids have been treated as liquids and observed in continuous shear. The present paper describes a concentric cylinder creep apparatus designed to enable viscoelastic parameters to be measured. A resumé of current theory is given and some experimental data analysed.

IT has become obvious in recent years that pharmaceutical preparations such as creams and pastes are complex rheological bodies; e.g. they exhibit viscoelasticity (linear and non-linear). Until recently these viscoelastic properties have been ignored, and continuous shear experiments have been made to measure such properties as hysteresis loop area and shear stress at a spur point in the shear stress-shear rate diagram. These experiments are used to examine the complex phenomenon of breakdown and classical parameters such as viscosity and elasticity are not measured directly. It is valuable both theoretically and practically to consider a system in the rheological ground state, that is without the method of testing significantly altering the structure, and to express the results of such tests in combinations of simple physical entities.

Many of the preparations used in pharmacy are multiphase where the phase boundaries are stabilized with complex films built from moderately low molecular weight components, e.g. Aqueous Cream B.P. Although historically the application of the theory of linear viscoelasticity has been most noticeable in the field of synthetic high polymers (Ferry, 1958, 1961a; Leaderman, 1958; Turner Alfrey & Gurnee, 1956) there is no fundamental reason why the theory should not be applied to the pharmaceutical systems mentioned above, and probably to many others.

The purpose of this paper is to present details of an apparatus which is designed to measure the necessary rheological parameters that are required to describe rheologically complex materials used in pharmacy. A resumé of current theory associated with linear viscoelastic behaviour is also given for the case of the creep test, that is deformation of the sample under constant stress.

Theory

LINEARITY OF RHEOLOGICAL BEHAVIOUR

Viscoelastic considerations can only readily be applied to a sample which has a linear strain response to an applied stress and vice versa. For any particular material there is a definite range of strain over which linearity holds.

From The School of Pharmacy, University of London, 29/39 Brunswick Square, London, W.C.1, England.

* Initial work on this apparatus formed part of a thesis accepted for the degree of Ph.D. in the University of London. Present address: School of Pharmacy, Portsmouth College of Technology, Portsmouth, Hants.

The requirements for linearity have been dealt with by Boltzmann (1876) and Van Wazer, Lyons & others (1963a). These are implicit in the principle of superposition which has the same mathematical form both in mechanical systems and electrical networks (Goldman, 1966). In mechanical terms, the principle of superposition states that if the system under investigation can be represented by a network of rheological models each of which has constant parameters, and if several stresses are applied either at the same or different times, then the total strain is equal to the sum of the strains produced by the stresses applied separately.

SPECTRA OF TIMES

A fundamental rheological parameter of a simple viscoelastic solid is the retardation time. This may be defined as the ratio of viscosity to shear elasticity in the sample. A complex viscoelastic solid would have to be represented by more than one retardation time.

An experimental set of data of total shear strain $\gamma(t)$ at constant applied stress ($=\sigma_1$) such that

$$J(t) = \frac{\gamma(t)}{\sigma_1}$$

may be analysed in two ways, either to give a continuous spectrum of retardation times or a line spectrum of retardation times (Ferry, 1961b). The choice of analysis really depends on the number and spacings of retardation times in the system under investigation. Resolution of individual retardation times is made difficult or impossible if the number is greater than ten and the smallest spacing between any two adjacent retardation times is less than five times the value of the smaller retardation time. In such a case the continuous spectrum method is most tractable, but for fewer retardation times a more accurate representation would be the use of a line spectrum.

The number of retardation times in an experimental system will depend on the degree of parity between the various ratios of bond energy to bond modulus for the various entities present (Lethersich, 1949). If the degree of parity is good (e.g. in simple fluids such as water and ethanol) the number of retardation times will be small. However if the above ratios extend over a wide range, the number of retardation times may be immense (e.g. aqueous solutions of high molecular weight cellulose ethers).

The range of these ratios will in turn depend on several factors: (*a*) The size of the particles or molecules involved. (*b*) Their shape (large or small aspect ratio). (*c*) The number of molecules or particles taking part.

In general the range of ratios will be small for low molecular weight species and for particles or molecules which are nearly spherical or ellipsoidal in shape.

The authors suspect that many pharmaceutical emulsions, creams, suspensions and pastes have component parameters which would yield a fairly simple line spectrum analysis. It should be noted that the most complicated cases are those involving high molecular weight thread like molecules, made up of components of widely differing molecular weights.

Here, factors (*a*), (*b*) and (*c*) mentioned above give rise to a complicated spectrum of retardation times. A continuous spectrum of retardation times is commonly calculated for these systems (Ferry, 1961b).

Sometimes, where the spectrum of retardation times extends over several factors of ten of time, it is possible that only part of the spectrum may be determined due to the time scale of the experiment. The present apparatus does not give useful data for determination of times less than 30 sec.

DERIVATION OF SHEAR BEHAVIOUR IN TERMS OF SERIES VOIGT MODEL ELEMENTS UNDER CONSTANT STRESS

The apparent time dependent shear compliance J(t)* of a linear viscoelastic solid or semi-solid may be represented by the algebraic sum of a set of hypothetical series compliances which may or may not have a direct physical significance in the system of interest (Karas & Warburton, 1961).

Thus
$$J(t) = \sum_{i=0}^{n} J_i(t) \qquad (1)$$

It is also demonstrable that these systems can also be represented by a set of parallel time dependent moduli such that

$$G(t) = \sum_{r=0}^{n} G_r(t) \qquad (2)$$

However, data obtained under constant stress conditions (creep) are more readily analysed using equation (1).

In the essentially solid system each individual contributory compliance $J_i(t)$ is a function of time and in the most elementary case may be represented by a Voigt model (Van Wazer & others, 1963b). The Voigt model consists of an elastic element and a viscous element coupled in parallel. In shear, the appropriate moduli involved are the shear modulus G_I and the shear or Newtonian viscosity η_I. If σ_I is the total constant shear stress

$$\sigma_I = \gamma_I G_I + \frac{d\gamma_I}{dt}\eta_I \qquad (3)$$

by using Hooke's and Newton's laws. Re-arranging equation (3)

$$\frac{d\gamma_I}{\sigma_I - \gamma_I G_I} = \frac{1}{\eta_I} dt \qquad (4)$$

If the retardation time for the 'i'th element is defined as

$$\tau_I = \frac{\eta_I}{G_I} \text{ or } \eta_I J_I$$

equation (4) becomes

$$\frac{d\gamma_I}{\frac{\sigma_I}{G_I} - \gamma_I} = \frac{dt}{\tau_I} \qquad (5)$$

* All symbols are defined in Appendix 1, p. 268.

On integration without limits

$$-\ln\left\{\frac{\sigma_1}{G_1}-\gamma_1\right\}=\frac{t}{\tau_1}+k_1 \quad .. \quad .. \quad .. \quad (6)$$

At the start of the experiment $t=0$, $\gamma_1=0$; thus:

$$k_1=-\ln\{\sigma_1 J_1\};\ \ln\left\{\frac{\sigma_1 J_1-\gamma_1}{\sigma_1 J_1}\right\}=-\frac{t}{\tau_1} \quad .. \quad (7)$$

$$\gamma_1=\sigma_1 J_1\left\{1-e^{-t/\tau_1}\right\} \quad .. \quad .. \quad .. \quad (8)$$

$$J_1(t)=J_1\left\{1-e^{-t/\tau_1}\right\} \quad .. \quad .. \quad .. \quad (9)$$

Compliances connected in series are additive so:

$$J(t)=\sum_{i=0}^{n} J_i\left\{1-e^{-t/\tau_1}\right\} \quad .. \quad .. \quad (10)$$

It is usual to assume also, for a real material, that the spectrum of values of τ_1 can include at the limits $\tau_1=0$ and ∞.

In the first case ($\tau_1=0$) the Voigt model reduces simply to an elasticity of compliance J_0 and in the second case ($\tau_1=\infty$) the Voigt model reduces simply to a viscosity of compliance t/η_0. In this way the treatment can be extended to cover viscoelastic liquids:

$$\eta_0\frac{d\gamma_\eta}{dt}=\sigma_i \quad .. \quad .. \quad .. \quad .. \quad (11)$$

Integrating:

$$\gamma_\eta=\frac{\sigma_1 t}{\eta_0}+k_2;\ t=0,\ \gamma_\eta=0,\ k_2=0$$

Hence:

$$J_{\eta_0}(t)=\frac{t}{\eta_0} \quad .. \quad .. \quad .. \quad (12)$$

For a line spectrum

$$J(t)=\sum_{i=0}^{n} J_i\left\{1-e^{-t/\tau_1}\right\}+\frac{t}{\eta_0};\ (\tau_0=0) \quad .. \quad (13)$$

In equation (13) the residual instantaneous shear compliance J_0 is regarded as being contained in the summation term. Mathematically it is not useful to include $J_{\eta_0}(t)$ in the summation term.

LINE SPECTRUM ANALYSIS OF CREEP RESULTS

Rheological creep data may be subjected to a stepwise analysis to yield discrete pairs of values of J_1, τ_1 for n models. It is usual to start the analysis of the creep data, starting with data collected at long times in the experiment. The analysis is conveniently divided into a number of steps.

Step 1. It must first be decided whether $J_{\eta_0}(t)$ is zero, finite or infinite: normally some intermediate state $0 < J_{\eta_0} < \infty$ is observed for a real material. Whichever of the three conditions apply, a plot of J(t) against time will produce one of the three curves shown in Fig. 1. Equilibrium or steady state is reached when a straight line portion of the plot is attained. This condition determines the suitable duration of the experiment.

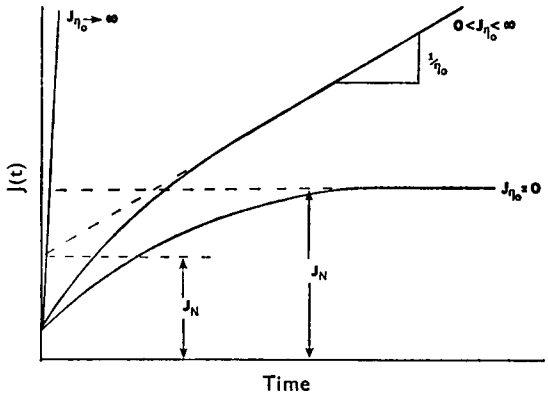

FIG. 1. Theoretical creep curves. For symbols see Appendix 1, p. 268.

It may be assumed for the purpose of the analysis that when the linear portion of the plot is reached all the component Voigt models present in the representation are fully extended:

$$J_i(t = \infty) = J_i \qquad 1 \leqslant i \leqslant n$$

From equation (13) the slope of the linear region of the graph is $1/\eta_0$ and so η_0 is obtained. Since the contribution to the creep compliance of $J_{\eta_0}(t)$ is now known, $(J(t) - J_{\eta_0}(t)$; 13a) is calculated. The contribution to the total creep compliance of the models can be calculated in turn starting with the one of largest retardation time τ_n.

Step 2. For the general Voigt model, equation (9) may be rewritten to give:

$$\frac{J_i - J_i(t)}{J_i} = e^{-t/\tau_i} = R_i(t) \qquad .. \quad .. \quad (14)$$

$$J_i(t) = \{1 - R_i(t)\} J_i \qquad .. \quad .. \quad .. \quad (15)$$

$$\text{Let} \sum_{i=0}^{n} J_i = J_N \quad .. \quad .. \quad .. \quad .. \quad .. \quad (16)$$

$$J(t) = \sum_{i=0}^{n} \{1 - R_i(t)\} J_i + J_{\eta_0}(t) = J_N - \sum_{i=0}^{n} R_i(t) J_i + J_{\eta_0}(t) \qquad (17)$$

After a certain time from loading all models except the nth may be considered to be essentially fully extended (for absolute maximum extension, infinite time would be required) so:

For $t \gg \tau_n$, $\sum_{i=0}^{n-1} R_i(t)J_i = 0$

$$J(t) = J_N - R_n(t)J_n + J_{\eta_0}(t) \quad .. \quad .. \quad (18)$$

For the experimental data as calculated at 13a the following parameter is evaluated

$$Z_n = \frac{J_N - J(t) + J_{\eta_0}(t)}{J_N} \quad .. \quad .. \quad (19)$$

The quantities of interest, but not directly available, however, are J_n, τ_n and $R_n(t)$. (17), (18) and (19) give:

$$R_n(t) = \frac{Z_n J_N}{J_n} \quad .. \quad .. \quad .. \quad (20)$$

From (14) and (20)

$$-\frac{t}{\tau_n} = \ln Z_n + \ln \frac{J_N}{J_n} \quad .. \quad .. \quad (21)$$

Thus a plot of $\ln Z_n$ against t gives a straight line of slope $-1/\tau_n$ for $t \gg \tau_n$. See example (Fig. 4). For $t \leqslant \tau_n$, the data will not lie on the extrapolated line. The latter makes an intercept of $-\ln (J_N/J_n)$ on the $\ln Z_n$ axis.

Since J_N is known J_n can be calculated.

Step 3. The values of $J_n(t)$ are now evaluated from the determined values of J_n and τ_n for all values of t and subtracted from the corresponding values of $J(t) - J_{\eta_0}(t)$.

The residuals now represent

$$\sum_{i=0}^{n-1} J_i \left\{1 - e^{-t/\tau_i}\right\}$$

It is now possible to return to the beginning of Step 2 and treat the processed data once more.

Equation (19) is now replaced by

$$Z_{n-1} = \frac{J_{N-1} - J'(t)}{J_{N-1}} \quad .. \quad .. \quad .. \quad (22)$$

where $J_{N-1} = J_N - J_n$

$$J'(t) = J(t) - J_n(t) - J_{\eta_0}(t)$$

but the process is unaltered in principle. Successive repetitions of

Steps 2 and 3 yield J_{n-1}, τ_{n-1}, J_{n-2}, τ_{n-2} etc. until the data is exhausted. The approximation is made that the remaining points at short times (see dotted line, Fig. 5) are due to one further Voigt unit. Any remaining compliance is approximated to a residual compliance referred to as J_0. However, a high frequency oscillation experiment might allow this J_0 to be resolved into further pairs of J_1, τ_1 values.

TRUE VALUE OF J_N

The accuracy of the whole analysis depends on the best fit value of J_N. This is the equilibrium or steady state value because t approaches infinity and is not readily accessible experimentally.

The best fit value of J_N in practice has to be guessed in a series of approximations before the first model can be evaluated.

Differential approach. Another method of estimating J_N is from the slope of the J(t) versus t plot in the curved region of Fig. 1 before the final linear region.

In this region

$$J(t) - J_{\eta_0}(t) = J_{N-1} + J_n\left\{1 - e^{-t/\tau_n}\right\} \quad .. \quad .. \quad (25)$$

where

$$J_N \simeq J_{N-1} + J_n \quad .. \quad .. \quad .. \quad (26)$$

On differentiation:

$$\frac{d\{J(t) - J_{\eta_0}(t)\}}{dt} = \frac{1}{\tau_n} \cdot J_n.e^{-t/\tau_n} \quad .. \quad .. \quad (27)$$

from which J_n and τ_n are readily accessible.

Intrinsically, this is the more accurate method, although it depends on experimental data of a high order of precision for the evaluation of

$$\frac{d\{J(t) - J_{\eta_0}(t)\}.}{dt}$$

An alternative method of the treatment of line spectrum analysis of creep results has been given by Inokuchi (1955), Sharma & Sherman (1966) and Sherman (1966).

Experimental

GENERAL ARRANGEMENT

Since many pharmaceutical preparations are of a liquid or soft gel-like consistency, it is very often difficult to obtain sufficient coupling through a sample to make rheological measurements in cone and plate or parallel plate geometry. If the diameter of the cone and plate is increased to obtain more torque, eventually the edge gap becomes so wide that the material easily flows out of the gap. Alternatively, if the cone angle is decreased the angular movement for any particular strain is reduced, leading to measuring difficulties. There is also the attendant and serious problem

of evaporation of water from emulsions and creams of the oil-in-water type.

The apparatus described is a concentric cylinder creep device built as a modification to the Weissenberg Rheogoniometer (Sangamo Controls Ltd.*). This is shown in Fig. 2a. The concentric cylinder geometry is particularly effective in overcoming the problems of lack of sample coupling and evaporation of water. There is a large area available for providing torque but only a small area from which water may evaporate. The concentric cylinders are made of stainless steel. The outer cylinder is machined with an annular trough to hold water and is located by means of two stainless steel pins which fit into a Perspex disk adapter. This adapter is screwed into the top cap flange of the fixed vertical stub shaft of the rheogoniometer (which is available from the manufacturers for rotational work not involving the measurement of normal force).

The Perspex disk reduces heat loss from the outer cylinder and sample into the large heat sink of the base of the rheogoniometer. The inner cylinder is hollow to reduce weight and end correction and a shallow angled nylon cone can be fitted to close the end if required. For greater accuracy, the end correction may either be eliminated (Couette, 1890, Hatschek, 1913, Mooney & Ewart, 1934, Mooney, 1946, Turner Alfrey & Rodewald, 1949, Moore & Davies, 1956) or calculated (Dinsdale & Moore, 1962, Lillie, 1930, Lindsley & Fischer, 1947). The inner cylinder is attached to an air bearing rotor by a short rod which also supports a Perspex shield. The latter, being cylindrical and of a diameter equal to the mean diameter of the trough described above, can be adjusted just to dip into the water when the inner cylinder is lowered into the outer cylinder. A vapour seal is thus provided, reducing evaporation from the sample.

In using the apparatus, the drag on the shield of the water in the trough will appear as an error in the results. This is usually negligible, but may be relatively more important with samples of low viscosity, in which cases the shield may be adjusted to a position just clear of the water surface. This arrangement still functioned efficiently as a humidity chamber.

The top of the air-bearing rotor carries the 10 cm arm to the transducer (Bolton Paul Meter Type C51) and above this is fitted a fixed grooved wheel of diameter 4·00 cm about which the torque may be applied.

APPLICATION OF TORQUE

The necessity of reproducing an accurately defined torque of suitable value in the horizontal plane in this type of apparatus confronts the experimenter with a particularly difficult problem. The most convenient source of force of constant magnitude which is independent of distance of application is the action of the earth's gravitational field on a fixed mass. However, this acts in a vertical plane. The line of action of an applied force may be turned through a right angle by means of a string

* Sangamo Controls Ltd., North Bersted, Bognor Regis, Sussex, England.

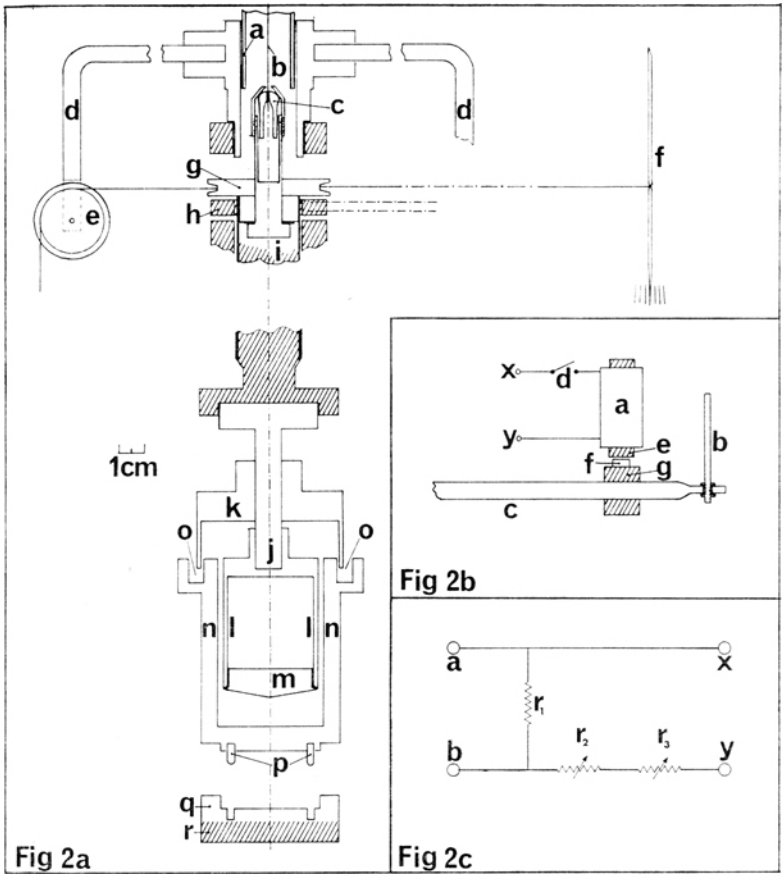

FIG. 2. **a.** Section of creep apparatus. Key: a. Lower part of 66 cm long support cylinder. b. 0·015 cm diam. beryllium-copper wire. c. Chuck, gripping the beryllium-copper wire. d. Stainless steel arms supporting the pulleys e. e. Pulley wheels (only the left-hand one shown) for loads greater than 5 g. f. Chemical balance pointer arm, showing the notched point. g. 4 cm diameter grooved wheel for torque application. h. Collet holding transducer arm (transducer arm is shown dotted, although not in the same plane as the drawn section). i. Upper part of air-bearing rotor. j. Rod, supporting the inner cylinder. k. Perspex shield. l. Inner cylinder. m. Shallow-angled nylon cone, closing inner cylinder. n. Outer cylinder. o. Annular trough in top of outer cylinder. q. Perspex disk, supporting outer cylinder. r. Steel base disk, existing part of rheogoniometer. Hatched areas of the section represent existing components of rheogoniometer. Water jacket not shown.

b. Quick release mechanism. Key: a. Electromagnet. b. Transducer core. c. Transducer arm. d. Switch for immediate application of stress to sample. e. Core of electromagnet. f. Brass stud. g. Armature. Power supply, 12 V., 50 cycles, is applied at x-y.

c. Recorder attenuating network. R_1 is a high stability fixed resistor of 1·8 ohms, R_2 and R_3 are wire wound resistances of maximum values 250 and 25 ohms respectively. Terminals a and b are connected to the Kent Recorder and x and y to the Boulton Paul meter.

passing over a pulley. For high torques, two opposed pulleys have been used with half the applied load in each pan, but even with the best types of pulley, at low applied forces, static friction losses in the bearings may account for variable force losses of up to 5% of that applied.

The laboratory balance has been used as a device which enables the required transformation of force to be accomplished without measurable losses at low torques. The applied torque to the inner cylinder of the creep apparatus is produced by the horizontal tension in a string between the balance pointer arm and the 4 cm grooved wheel described above. The string naturally falls into a catenary even when under tension but only the horizontal component is effective in providing a horizontal torque on the inner cylinder and this is equal in magnitude to the horizontal component at the pointer. The string is attached to the balance pointer at the notched point, f, Fig. 2a. The distance between the notched point of the pointer arm and the main balance knife-edge is made exactly half the outer knife-edge interdistance. In this way a one-to-one ratio is obtained in the conversion of force through a right angle. Hence if a mass of M g is placed in the left hand balance pan a torque of 2Mg dyne cm is applied to the inner cylinder of the apparatus when the balance is raised. The one-to-one ratio of forces is only strictly maintained when the pointer arm of the balance is on the centre zero. This condition is achieved either by making a small adjustment in the distance between the balance and the rheogoniometer or by the addition of small masses to the centre of the string.

QUICK RELEASE MECHANISM

It is essential in creep experiments to apply the constant stress during a very short period of time (theoretically instantaneously) and then maintain it constant during the experiment. It was found using the present equipment that it was not possible to achieve reproducible initial loading by simply raising the balance arm.

The electromagnetic release mechanism shown in Fig. 2b was devised to this end. A small soft iron armature is clamped to the mid point of the 10 cm transducer arm and is normally held stationary by an electromagnet which is energized by 50 cycle AC. The armature is held away from the soft iron core of the electromagnet by the small brass stud to ensure that a residual magnetic circuit cannot remain when the current is switched off.

An experiment is normally started by first energizing the electromagnet then raising the balance arm and finally cutting the current to the electromagnet. The stress is applied to the sample at the instant of de-energizing the electromagnet.

SUSPENSION ARRANGEMENTS FOR THE INNER CYLINDER

Attached to the 4 cm diameter grooved wheel at the top of the inner cylinder is a chuck which grips a beryllium-copper wire, the other end of which is soldered into an adjustable boss situated at the upper end of a 66 cm long support cylinder. This cylinder, at the lower end, fits into the

top of the rheogoniometer head and is clamped in the same manner as a standard torsion bar. The air bearing, which is practically frictionless and which maintains the axis of the inner cylinder against side thrusts produced by the applied torque, has been used by Oldroyd, Strawbridge & Toms (1951). The beryllium-copper wire has a diameter of 0·015 cm and was annealed for 3 hr at 320°. The torque produced by this wire during a typical creep experiment (when the applied torque was $9{\cdot}6 \times 10^3$ dyne cm) was so low that the variation in applied torque during the experiment due to the wire was not more than $7{\cdot}3 \times 10^{-4}$ %. Although the wire has to support the whole of the inner cylinder assembly, a load of 650 g, it was found that a 1 kg load was still within the elastic limit for the wire. This condition is essential so that the inner cylinder should not ground at the bottom during a run and also that the core of the stress-transducer should not become misaligned. The boss at the top of the supporting tube is adjustable in position so that the relative height of the inner cylinder assembly can be adjusted independently of the rheogoniometer lead-screw.

THERMOSTAT

A constant temperature water bath passes water through a jacket (fitted with a thermometer, 0·1° divisions) which surrounds the outer cylinder. So that the apparatus could in future also be used as a normal coaxial cylinder viscometer, it was manufactured so that a gap was left between the inner surface of the constant temperature jacket and the outer surface of the cylinder, i.e. the outer cylinder could be rotated by the rheogoniometer motors if required. However for the present work a brass tube, lubricated with silicone grease, was inserted to fill the gap; this decreases the time required for temperature equilibration to take place.

RECORDING ARRANGEMENTS

The output of the Boulton Paul Meter Type C51 is connected to a single point Kent recorder by means of an attenuating network, shown in Fig. 2c.

R_2 (coarse) and R_3 (fine) are adjusted to give full scale deflection on the Kent recorder with the Boulton Paul meter switched to CAL.

METHOD FOR CREEP TESTING

The general procedure is as follows. A sample is placed into the outer cylinder and the inner cylinder is slowly lowered until its top is level with the top of the outer cylinder. The excess material is removed and the vapour shield placed in position to minimize evaporation; the apparatus is left overnight for the temperature to equilibrate and for any stresses in the sample to relax.

Immediately before a run is made, most of the water in the outer cylinder trough is removed with a hypodermic syringe. A constant stress is then suddenly applied to the sample as described in a previous section.

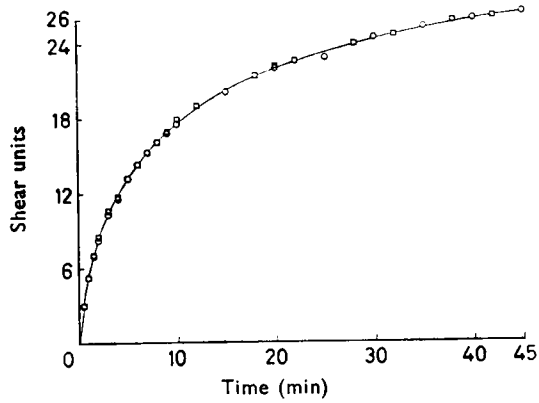

FIG. 3. Experimental and theoretical creep shear data as functions of time. □ — Experimental points ○ — Theoretical points.

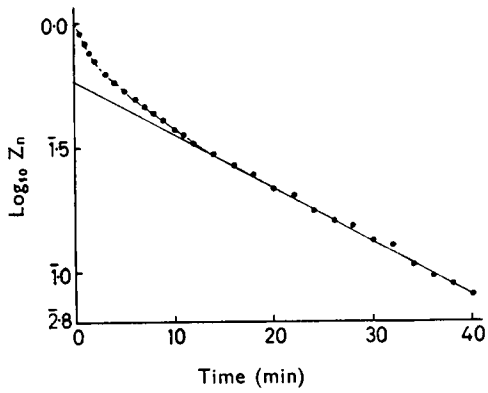

FIG. 4. Plot of $\log_{10} Z_n$ against time.

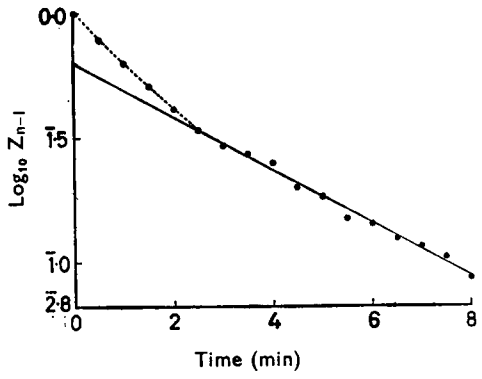

FIG. 5. Plot of $\log_{10} Z_{n-1}$ against time.

EXAMPLE OF TREATMENT OF RESULTS

The following set of data (Barry, 1967) is analysed according to the above theoretical treatment.

A plot of the experimental shear data versus time in minutes is given in Fig. 3. The shear units plotted are 0·1 mV units of the 12 mV Kent Recorder used. A deflection 0·1 mV is equivalent to a sample shear of $17{\cdot}98 \times 10^{-4}$. It will be noted that the initial instantaneous deflection due to the unshunted shear compliance J_0 and the continuous steady shear rate due to the unshunted viscosity η_0 have already been subtracted. The shear stress used in the experiment is 79·8 dynes cm^{-2}. The theoretical points shown in Fig. 3 are calculated from the derived components of the total viscoelastic model given in Table 1. The agreement is good.

Fig. 4 shows the second stage of the analysis where $\log_{10} Z_n$ is plotted against time. The use of logarithms to the base ten is more convenient, in practice, than the use of natural logarithms and the correct value of τ can be calculated from the slope of the best straight line using the necessary conversion factor for logarithms to different bases. Fig. 5 shows a further stage where $\log_{10} Z_{n-1}$ is plotted against time.

The values of the components of the total viscoelastic model are given in Table 1.

TABLE 1. VALUES OF VISCOELASTIC PARAMETERS

Voigt unit i value	τ (sec)	J($cm^2 dyne^{-1}$)	$\eta = \tau \times \frac{1}{J}$ (poise)
(J) 0	—	$4{\cdot}22 \times 10^{-5}$	—
1	$1{\cdot}23 \times 10^3$	$9{\cdot}35 \times 10^{-5}$	$1{\cdot}32 \times 10^7$
2	$2{\cdot}45 \times 10^3$	$4{\cdot}15 \times 10^{-5}$	$5{\cdot}91 \times 10^6$
3	$5{\cdot}88 \times 10$	$2{\cdot}47 \times 10^{-5}$	$2{\cdot}38 \times 10^6$
(η) 0	—	—	$2{\cdot}38 \times 10^7$

The creep shear compliance J(t) was calculated as follows:

Using the well-known expression for concentric cylinders (Dinsdale & Moore, 1962)

$$G(t) = \frac{T}{4\pi h}\left(\frac{1}{R_1^2} - \frac{1}{R_2^2}\right)(\theta(t))^{-1}$$

it follows that:

$$J(t) = \frac{4\pi h}{T}\left(\frac{1}{R_1^2} - \frac{1}{R_2^2}\right)^{-1}\theta(t)$$

Where the important dimensions of the cylinders and gap are: R_1 = radius of inner cylinder = 1·84 cm; R_2 = radius of outer cylinder = 2·10 cm; h = height of inner cylinder = 5·0 cm; T = applied torque (dyne cm); θ = angular deflection of inner cylinder (rads.); G(t) = 1/J(t).

Acknowledgements. The authors wish to thank Dr. K. Ridgway for suggesting the use of the chemical balance for the application of low torques, and Mr. J. Deer for help with the design and construction of the apparatus.

APPENDIX 1

List of symbols used:

σ_i = shear stress applied to the 'i'th Voigt model
γ_i = shear strain of the 'i'th Voigt model
$\frac{d\gamma_i}{dt}$ = rate of shear strain of the 'i'th Voigt model
$\gamma(t)$ = total shear strain at time t
G_i = shear modulus of the 'i'th Voigt model
η_i = shear viscosity of the 'i'th Voigt model
$J_i = {}^1/G_i$ = shear compliance of the elastic part of the 'i'th Voigt model
$J_i(t)$ = the apparent shear compliance at time t of the 'i'th Voigt model
J_o = unshunted or residual shear compliance
η_o = unshunted or residual shear viscosity
t = time in sec
J_N = total creep compliance at equilibrium
J(t) = total creep compliance at time t
$J\eta_o(t)$ = equivalent compliance of η_o at time t
τ_i = retardation time of the 'i'th Voigt model
$R_i(t)$ = compliance normalizing factor for the 'i'th Voigt model = e^{-t/τ_i}
Z_n = compliance parameter defined by equation (19)

References

Barry, B. W. (1967). Ph.D. Thesis, University of London, 179–186, 198.
Boltzmann, L. (1876). *Pogg. Ann. Phys.*, 7, 624.
Couette, M. (1890). *Annls Chem.*, **21**, 433–510.
Dinsdale, A. & Moore, F. (1962). *Viscosity and its Measurement*, pp. 27–46, London: Chapman & Hall.
Ferry, J. D. (1958). *Rheology, Theory and Applications*, Vol. 2, pp. 433–473, editor Eirich, F. R., London: Academic Press.
Ferry, J. D. (1961a). *Viscoelastic Properties of Polymers*, London: John Wiley.
Ferry, J. D. (1961b). *Ibid.*, p. 45.
Goldman, S. (1966). *Laplace Transform Theory and Electrical Transients*, p. 107, New York: Dover Publications.
Hatschek, E. (1913). *Trans. Faraday Soc.*, **9**, 80–92.
Inokuchi, K. (1955). *Bull. chem. Soc. Japan*, **28**, 453–465.
Karas, G. C. & Warburton, B. (1961). *Br. Plast.* (March 1961), 4–5.
Leaderman, H. (1958). *Rheology, Theory and Applications*, editor Eirich, F. R., Vol. 2, pp. 1–61, London: Academic Press.
Lethersich, W. (1949). *Electrical Research Association Technical Report No.* LT1864, pp. 5–8.
Lillie, H. R. (1930). *Phys. Rev.*, **36**, 347–362.
Lindsley, C. H. & Fischer, E. K. (1947). *J. appl. Phys.*, **18**, 988–996.
Mooney, M. (1946). *J. Colloid Sci.*, **1**, 195–208.
Mooney, M. & Ewart, R. H. (1934). *Physics*, **5**, 350–354.
Moore, F. & Davies, L. J. (1956). *Trans. Br. Ceram. Soc.*, **55**, 313–338.
Oldroyd, J. G., Strawbridge, D. J. & Toms, B. A. (1951). *Proc. phys. Soc.*, **64B**, 44–57.
Sharma, F. & Sherman, P. (1966). *J. Food Sci.*, **31**, 699–706.
Sherman, P. (1966). *Ibid.*, **31**, 707–716.
Turner Alfrey, T. Jr. & Gurnee, E. F. (1956). *Rheology, Theory and Applications*, editor Eirich, F. R., Vol. 1, pp. 387–429, New York: Academic Press.
Turner Alfrey, T. Jr. & Rodewald, C. W. (1949). *J. Colloid Sci.*, **4**, 283–298.
Van Wazer, J. R., Lyons, J. W., Kim, K. Y. & Colwell, R. E. (1963a). *Viscosity and Flow Measurement. A Laboratory Handbook of Rheology*, p. 362. London: Interscience,
Van Wazer, J. R., Lyons, J. W., Kim, K. Y. & Colwell, R. E. (1963b). *Ibid.*, p. 350.